[Article ID] 1003 - 6326(2002) 06 - 1195 - 04

# Chemical reaction model of cathode failure in large prebaked anode aluminum reduction cells ①

ZHAO Qun(赵 群) [1], XIE Yan-li(谢雁丽) [1], GAO Bing-liang(高炳亮) [1], QIU Zhu-xian(邱竹贤) [1], ZHAO Wu-wei(赵无畏) [2]

(1. School of Materials and Metallurgy, Northeastern University, Shenyang 110004, China;
2. Zhengzhou Light Metals Research Institute, Zhengzhou 450041, China)

**[Abstract]** By partial and general dissection of large prebaked alumina electrolysis cells, the macro appearance, chemical composition and phase variations were studied employing actual observations and measurements on the cells together with X-ray diffraction phase analysis and scanning electron microscopy of samples from different locations. According to the practical production, a chemical reaction model of aluminum reduction cell failure was set up in order to reduce the incidence of cell failure and extend pot service life.

**[Key words]** cathode failure, chemical reaction model, large prebaked cell, pot service life

**[CLC number]** TF 821 **[Document code]** A

## 1 INTRODUCTION

In the recent five years, a number of large capacity cells, such as 320 kA, 280 kA, 200 kA, 190 kA, etc, were put on commercial use and the aluminum output will reach 500~ 600 tons per year after ten years. In this case, the cell life is extremely important for aluminum industry since it affords an overall indicator of technical and economic performance in aluminum smelting. In theory, pot life can amount to 10 or more years under standard conditions. In practice, the average service life of an industry cell is usually 3 to 6 years[1,2]. The gap is caused by pot failure occurred in working situation, such as the side lining and cathode failure usually led to cell run out and shut down. Many papers described the phenomenon but the analysis of the causes was not deep and completed enough[3,4]. In this paper, a damaged industrial 140 kA center-fed prebake cell was taken as an example, being completely cut-away to make samples. By practical observation on composition and phase analysis of samples, the cathode failure is studied and the chemical reaction model is set up to understand cathode failure and support theory basis to extend pot service life.

## 2 CATHODE STRUCTURE OF LARGE PREBAKED ALUMINUM REDUCTION CELL AND ITS FAILURE

At present, there are many types of large prebake aluminum reduction cell in China, but the cathodes have little difference. Most cathode, as well as sample cell in this paper, can be described as follows from up to down: using hot-rammed fine carbon block, standard length semi-graphitised carbon blocks are assembled on steel bar, and the peripheral seams and carbon block seams are cemented with cold-rammed carbon paste so that the bottom blocks and the single side block layer are connected to form an integral carbon inner lining. Heat-resistant concrete is cast around the steel bars, and refractory bricks are used to construct the mantle. The insulating layer is made up of light insulating bricks, an impermeable steel plate and alumina powder, together with refractory bricks. The expansion joint is filled with alumina powder.

The longer the cell worked, the harder the cathode failure happened, until the cell run out and shut down. By careful observation of broken cell, the cathode failure can be described as follows: bulging of pot bottom; breakage and splitting of carbon blocks; ablation pits; peripheral seam aliquation; steel bar fusion break or melting; grayish white layer formation and outward expansion of pot shell, etc. Samples with different appearances from different parts were taken and analyzed to find out cathode failure principles.

## 3 PHASE DETERMINATION AND MICROSTRUCTURE OBSERVATION

The broken cells were subjected to complete dissection by the dry pot cut-out method, and the phases in the materials were studied by measurement and sampling. By X-ray diffraction analysis, scanning electron microscopy and optical stereomicroscopic examination, the phase structure and composition, the microcrystalline status of samples in different locations are basically elu-

① [Received date] 2001 - 11 - 12 ; [Accepted date] 2002 - 04 - 05

cidated to provide basis on which to study chemical corrosions in lining and mechanism of cathode failure. The locations and appearance character of samples are described in Table 1.

The phase analysis of seven samples were done individually, the results and microcrystalline status of samples are illustrated as follows(seven X-ray diffraction patterns were omitted):

Phases of N1 are: $Na_3AlF_6$, $CaF_2$, $\beta$-$Al_2O_3$, graphite, NaF, $\alpha$-$Al_2O_3$ and $Al_4C_3$. The NaF crystals observed in SEM are hexagonal plates(see Fig. 1(a)) of about 1 $\mu$m in thickness, the largest plates being 70 $\mu$m. The aluminum polycrystals are irregular in form. A small amount of $Al_4C_3$ crystals are also visible.

Phases of N2 are: $Na_3AlF_6$, $Al_4C_3$, $CaF_2$, graphite, a small quantity of NaF, and $\beta$-$Al_2O_3$. The cryolite content was greater than in N1, amount of graphite was small. The cryolite crystallized with a small amount of NaF in the sample surface layer to form acicular crystals, see Fig. 1(b).

Phases of N3 are: $Al_4C_3$, $Na_3AlF_6$, $\beta$-$Al_2O_3$, $CaF_2$, and a small quantity of graphite. The $Al_4C_3$ content was high and the crystals were coarse, possessing laminar cracks; the crystal was brittle and readily fragmented, see Fig. 1(c).

The N4 sample have a high content of $Na_3AlF_6$ phase, with less amount of $\beta$-$Al_2O_3$, $CaF_2$, $\alpha$-$Al_2O_3$, NaF and a small amount of $C_{32}Na$.

Phases of N5 are: $Al_5Fe_2$, $Al_3Fe$ and AlSiFe alloy.

Phases of N6 are: $Al_4C_3$, $Na_3AlF_6$, $CaF_2$, $\beta$-$Al_2O_3$, and small quantities of NaF and graphite. Some of the cryolite crystals were coarse. See Fig. 1(d).

Phases of N7 are: $\alpha$-$Al_2O_3$, $\beta$-$Al_2O_3$, $Na_3AlF_6$, $CaF_2$, and $NaAlSiO_4$. See Fig. 2(e).

## 4 CHEMICAL REACTION MODEL OF CATHODE FAILURE IN LARGE PREBAKE CELLS

According to analysis results and industrial practice, a chemical reaction mould of cathode failure is established and presented as follows[1, 5, 6]:

Under industrial electrolysis conditions, sodium irons and aluminum ions are capable of partial co-electrodeposition because of the similarity of their potentials. Moreover, thermite reaction can displace Na from NaF, part of this sodium escaping by vaporization and part permeating into the carbon block and continuously diffusing to form a thermally unstable intercalation compound $C_{12}Na$ or $C_{32}Na$ or $C_{64}Na$ as

$$32C(s) + Na(g) = C_{32}Na(s) \quad (1)$$

The sodium carbide product of reaction(1) is the main cause of carbon block sodium swelling and exfoliation. Therefore, precipitation of sodium must be kept to a minimum, and the carbon lining should be controlled at a high temperature of no less than 900 ℃ to create conditions under which no sodium intercalation compounds can exist; efforts must be made to maintain a 850 ℃ solid phase isotherm in the refractory brick layer at the bottom of the carbon blocks[7, 8].

The sodium introduce into the carbon structure undergoes the following reactions with the percolating electrolyte:

$$3Na(\text{in C}) + Na_3AlF_6(l) = 6NaF(s) + Al(l) \quad (2)$$

$$12Na(\text{in C}) + 3C(s) + 4Na_3AlF_6(l) = Al_4C_3(s) + 24NaF(l) \quad (3)$$

**Table 1** Sampling position in 140 kA industrial electrolysis cell and apparent characteristics of samples

| Sample | Sample position | Apparent characteristic and phase composition |
|---|---|---|
| N1 | In ablation pit cavity in carbon block | Grey-white botryoid agglomerate; outer layer chiefly white electrolyte; interior containing pale yellow $\beta$-alumina and golden yellow $Al_4C_3$ |
| N2 | In carbon block fissure | Distinct gray-white sintered kidney-shaped or stellate aluminum granules surface layer of gray-white electrolyte, interior comprising light yellow $\beta$-alumina and golden yellow $Al_4C_3$ |
| N3 | Interior of transverse split in carbon block | Golden yellow, partly red botryoid agglomerate of $Al_4C_3$ crystals; characterized chiefly by complete crystallization and high content |
| N4 | Near steel cathode bar | White crystalline NaF; relatively pure on aluminum slab side; no golden yellow material |
| N5 | AlFe alloy at bottom of carbon block | Silver white with metallic luster, chiefly aluminum-iron alloy with gray electrolyte distributed in small crevices |
| N6 | Between carbon block and steel bar | Red-yellow chalk, very loose texture, with golden yellow $Al_4C_3$ granules clearly visible; few aluminum granules |
| N7 | Grey-white layer between metalliferous layer and refractory brick | Grey-black sintered mass, compact and relatively brittle; color and degree of compaction distinctly laminar in distribution |

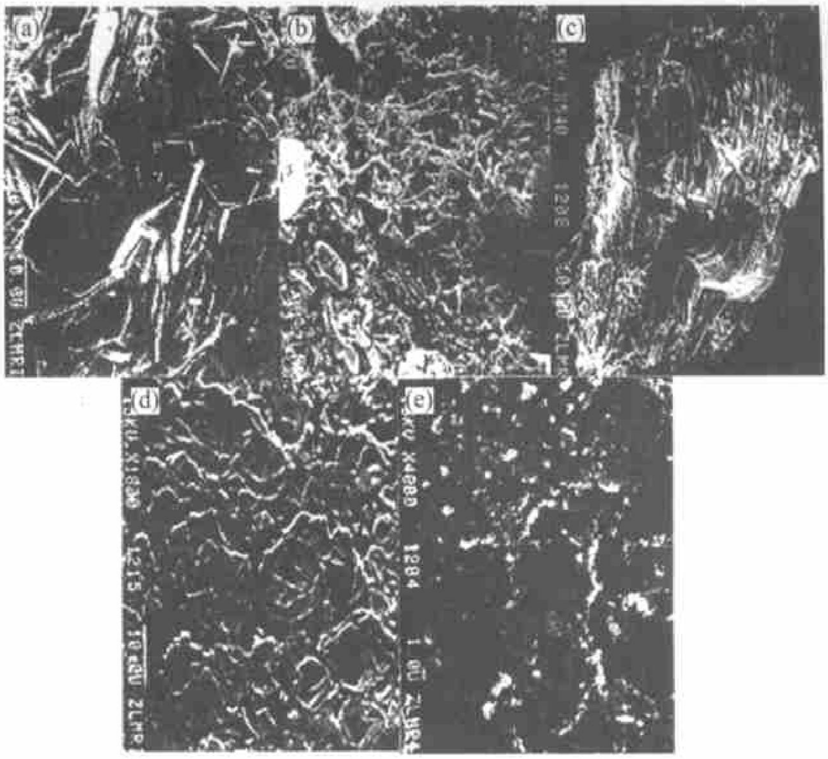

**Fig. 1** SEM results of samples
(a) —NaF; (b) —$Na_3AlF_6$(acicular); (c) —$Al_4C_3$; (d) —$Na_3AlF_6$(coarse); (e) —β-$Al_2O_3$

The volume of above reaction products are substantially increase compared with the reactants, hence widen the carbon block cracks, enlarge and deepen the pits, as a result accelerate carbon block failure. Analysis of samples collected from sampling position 6 and 7 illustrated that they contained pale yellow β-$Al_2O_3$ and α-$Al_2O_3$. The alumina is formed by the reaction as

$$6NaF(l) + 34Al_2O_3(dissolved) = 3Na_2O\cdot 11Al_2O_3(s) + 2AlF_3(l) \quad (4)$$

Owing to ingress of air, the following reactions also occur:

$$4Na(in\ C) + O_2(g) + 22Al_2O_3(s) = 2(Na_2O\cdot 11Al_2O_3) \quad (5)$$

$$12Na(in\ C) + 3O_2 + 4Na_3AlF_6(l) = 2Al_2O_3(s) + 24NaF(l) \quad (6)$$

$$2Na(in\ C) + 2C(s) + N_2(g) = 2NaCN(l) \quad (7)$$

$$8Na(in\ C) + 2FeO(s) + 13C + 6N_2(g) = 2Na_4Fe(CN)6(s) + CO_2(g) \quad (8)$$

$$2Al(l) + N_2(g) = 2AlN(s) \quad (9)$$

The above cyanides and nitride can hydrolyze in air, releasing the toxic gas HCN, and an ammoniac odor can be detected. Liquid aluminum leaked onto the steel bars reacts directly as

$$Al(l) + 3Fe(s) = AlFe_3(s) \quad (10)$$

In the presence of sodium, the reaction between the electrolyte and steel bars is

$$3Na(in\ C) + Na_3AlF_6(l) + 3Fe(s) = AlFe_3(s) + 6NaF(l) \quad (11)$$

The silvery white Al-Fe alloy layer 5 with a metallic luster is formed by this way. $Al_5Fe_2$, $Al_{13}Fe_4$ and AlFe-Si alloy phases were obtained from this material.

A layer of refractory brick in contact with the carbon cathode blocks is melted and corroded by the electrolyte, transforming to a grayish white layer and glassy compound (see phases of sample N7). The main compounds are α-$Al_2O_3$, β-$Al_2O_3$, NaF, $Na_3AlF_6$, $CaF_2$ and nephelite, formed by the reactions[9~11]:

$$8Na(g) + 5(3Al_2O_3\cdot 2SiO_2)(s) = 8NaAlSiO_4(s) + 2Si(s) + 11Al_2O_3 \quad (12)$$

$$8Al(g) + 3(3Al_2O_3\cdot 2SiO_2)(in\ solution) = 6Si(s) + 13Al_2O_3 \quad (13)$$

$$8NaF(l) + 5(3Al_2O_3\cdot 2SiO_2)(s) = 6NaAlSiO_4(s) + 2AlF_3(l) + 11Al_2O_3(s) + 5Al_2O_3 \quad (14)$$

$$3Na_3AlF_6(l) + 6(Al_2O_3\cdot 2SiO_2)(s) = 9NaAlSiO_4(s) + 2AlF_3(l) + 11Al_2O_3(s) + 3SiF_4(g) \quad (15)$$

The mullite in clay firebrick transforms to nephelite, and the nephelite reacts with the electrolyte, producing $SiF_4$, which escapes. The gaseous reaction product causes volume expansion of the grayish white layer formed by melting and transformation of the refractory brick, further aggravating upward bulge of the pot bottom.

Generally speaking, in industrial situation, the stresses created by sodium intercalation swelling inevitably act on the carbon block itself; the sodium atoms enter the crystal lattice and diffuse, causing the phase spacing of the carbon crystals to increase from its original $3.44 \times 10^{-10}$ mm to $3.71 \times 10^{-10}$ mm, leading to volume expansion and strength decrease in the carbon block. Since the excess thermal stress generated is necessarily released on all sides, the thermal stress remains after part of the excess thermal stress has been removed by outward expansion of the pot shell, which causes the carbon blocks to arch into a bulge, and then add to the crystallization pressure from molten salts percolating into the carbon gaps and apertures. The increased thickness of the Al-Fe alloy layer and grayish white layer serves to aggravate uplift of the whole pot bottom. When the heaving force exceeds the limit of flexure in the carbon blocks, the carbon blocks inevitably undergo compressive fracture and breakage, seriously damaging the carbon lining. The electrolyte sedimentation mixed with undissolved alumina constant swirl and scour the ablation pits, until the aluminum liquid and electrolyte make contact with the steel bars, damaging the bars by alloying and melting. At last, the cells run out and shut down.

## 5 CONCLUSION

As well as enduring physical and mechanical insult from stresses and abrasion, carbon cathode blocks of large prebake cells encounter chemical corrosion of many kinds under the action of heat, electrical, magnetic, fluid and mechanical force fields. Failure phenomena such as bulging, fracture, ablation pits and exfoliation of the cathode blocks are the result of the combined action of these deleterious factors. Using novel materials, such as anti-seep slip refractory, dry-barrier refractory, C-SiC composite lining and C-TiB cathode block, lining failure and bottom bulging can be reduced to extend the cell service life largely.

## [REFERENCES]


[1] QIU Zhu-xian, WANG Jia-qing, ZHENG Hong, et al (Transl). Alumina Electrolysis Cell Cathodes [M]. Shenyang: Editorial Office of Light Metals. 1991. 9.

[2] HUANG Yong-zhong. Aluminum Reduction Process [M]. Changsha: Central South University of Technology Press. 1993.

[3] QIU Zhu-xian, ZHANG Ming-jie. An investigation into the problem of cathode failure in industrial alumina electrolysis cells[J]. Light Metals, (in Chinese), 1991, 5: 57-61.

[4] YU Zong-yao. The causes of failure in 16 kA large prebake cell linings and improved methods of cell construction [J]. Light Metals, (in Chinese), 1991, 5: 62-67.

[5] YAO Guang-chun, QIU Zhu-xian. The chemical reactions occurring in alumina electrolysis cell lining [J]. Light Metals, (in Chinese), 1991, 5: 68-72.

[6] ZHANG Ming-jie. Study on Alumium Reduction Cell Service Life [M]. Shenyang: Northeastern University Press. 1991. 96-100.

[7] Vanvoren C, Homsi P, Basquin T L, et al. AP50: the pechiney 500 kA cell [J]. Light Metals, 2001, 16: 221-226.

[8] Tabereaux A T, Windfeld M. Evaluation and performance of power "dry-barrier" refractory for use in aluminum cell cathode [J]. Light Metals, 1995, 9: 471-477.

[9] Pawlek R P. SiC in aluminum electrolysis cell [J]. Light Metals, 1995, 9: 527-533.

[10] Tabereaux A T. Reviewing advances in cathode refractory materials [J]. JOM, 1992, 44(11): 20-21.

[11] HUANG Yong-zhong, LIU Ye-xiang, WANG Hua-zhang, et al. $TiB_2$-coating cathode in aluminum reduction cell [J]. The Chinese Journal of Nonferrous Metals, (in Chinese), 1996, 6(2): 19-22.


**(Edited by LONG Huai-zhong)**